International Journal of Biological Macromolecules 159 (2020) xxx

Contents lists available at ScienceDirect

International Journal of Biological Macromolecules

journal homepage: http://www.elsevier.com/locate/ijbiomac

Characterization and cytoprotective properties of *Sargassum natans* fucoidan against urban aerosol-induced keratinocyte damage

Ilekuttige Priyan Shanura Fernando [a,b], Kalu Kapuge Asanka Sanjeewa [b], Hyo Geun Lee [b], Hyun-Soo Kim [c], Andaravaas Patabadige Jude Prasanna Vaas [d,e], Hondamuni Ireshika Chathurani De Silva [d], Chandrika Malkanthi Nanayakkara [f], Dampegamage Thusitha Udayangani Abeytunga [d], Won Woo Lee [g], Dae-Sung Lee [c,*], You-Jin Jeon [b,h,**]

[a] Department of Marine Bio-Food Sciences, Chonnam National University, Yeosu 59626, Republic of Korea
[b] Department of Marine Life Science, Jeju National University, Jeju 690-756, Republic of Korea
[c] National Marine Biodiversity Institute of Korea, 75, Jangsan-ro 101-gil, Janghang-eup, Seocheon, Republic of Korea
[d] Department of Chemistry, University of Colombo, Colombo 3, Sri Lanka
[e] School of Natural Sciences, University of Tasmania, Private Bag 75, Hobart, Tasmania 7001, Australia
[f] Department of Plant Sciences, University of Colombo, Colombo 3, Sri Lanka
[g] Freshwater Bioresources Utilization Division, Nakdonggang National Institute of Biological Resources, Sangju 37242, Republic of Korea
[h] Marine Science Institute, Jeju National University, Jeju Self-Governing Province 63333, Republic of Korea

ARTICLE INFO

Article history:
Received 12 February 2020
Received in revised form 14 May 2020
Accepted 17 May 2020
Available online 20 May 2020

Keywords:
Fucoidan
Sargassum natans
Fine dust

ABSTRACT

The escalation of fine particulate matter (PM) air pollution has recently become a global concern. Evidence is fast accumulating on PM exposure-related skin damage. The present study explored the therapeutic potentials of fucoidan purified from *Sargassum natans* against damaging effects of PM exposure on human HaCaT keratinocytes. Fucoidan (SNF7) was purified from *S. natans* by an enzyme-assisted extraction and purified by anion exchange chromatography. SNF7 (≈50 kDa) was identified as a fucoidan containing 70.97% fucose and 36.41 ± 0.59% of sulfate. Treatment of fine dust from Beijing, China (CFD) increased intracellular ROS levels in HaCaT cells triggering DNA damage and apoptosis. Treatment of SNF7 dose-dependently attenuated CFD-induced surge of intracellular ROS levels in keratinocytes by increasing antioxidant defense enzymes. Moreover, SNF7 chelated metal ions Pb^{2+}, Ba^{2+}, Sr^{2+}, Cu^{2+}, Fe^{2+}, and Ca^{2+} coming from CFD. The results substantiated the potential therapeutic effects of SNF7 against CFD-induced oxidative stress. Further studies could promote SNF7's use as an active ingredient in cosmetics.

1. Introduction

Ambient particulate matter (PM) is a leading cause of morbidity in East Asian countries, including China, Korea, and Japan. It has now become a major concern in dermatological research as a causative agent that adversely affects human skin [1]. The effects on the respiratory system have widely been studied. According to the World Health Organization, PM contributes to 800,000 premature deaths every year, ranking it the 13th leading cause of mortality worldwide [2]. PM could consist of a variety of substances such as smog, soot, molds, pollen-like allergens, mineral dust from sandstorms, and exhaust gas from vehicles, industries, and coal-burning plants [3]. Polycyclic aromatic hydrocarbons, heavy metals, sulfates, and nitrate compounds are among the constituents of PM that may stimulate allergic and inflammatory responses in cells [4].

Recent epidemiological investigations have demonstrated the impact of ambient air pollutants on the development of inflammatory skin diseases such as acne, atopic dermatitis, and psoriasis [5,6]. Atopic dermatitis is one of the most common allergic skin disorders seen among children, as noted in a recent study from South Korea describing the contribution of PM to atopic dermatitis in children inhabiting urban areas [7]. Arguments on the effects of fine dust on human skin are still at a controversial stage, which suggests the need for extensive investigations of the mechanisms involved. Ahn [8] reported that PM can increase the oxidative stress in skin tissues leading to immunological dysregulations. Moreover, PM-induced ROS are reported to aggravate skin aging (wrinkles) by increasing elastosis marked by the production

Abbreviations: PM, Particulate matter; SN, crude polysaccharide from *Sargassum natans*; SNF7, SN fraction 7; CFD, China fine dust; DW, deionized water.

* Corresponding author.
** Correspondence to: Y-J. Jeon, Department of Marine Life Science, Jeju National University, Jeju 690-756, Republic of Korea.
E-mail addresses: daesung@mabik.re.kr (D.-S. Lee), youjin2014@gmail.com (Y.-J. Jeon).

https://doi.org/10.1016/j.ijbiomac.2020.05.132
0141-8130/

of various matrix metalloproteinases in skin fibroblasts and keratinocytes [9,10]. This results in irregular skin darkening by stimulating melanin production, a condition known as lentigines [11].

Marine natural products have received increased attention in recent biomedical research due to their potential wide-ranging biological functionality and unfamiliar structural characteristics [12]. The brown algae-derived sulfated polysaccharide, fucoidan, is at the center of many ongoing biomedical investigations. Fucoidans are reported to possess wide-ranging bioactivities such as antioxidant, anti-inflammatory, immunemodulatory, anticancer, anticoagulant, antimicrobial, and many others [13]. Fucoidan has a chemical structure comprising abundant 3 and 4-linked α-l-fucopyranose residues interspersed with numerous monosaccharide units [14]. Heterogenous attachment of sulfate groups to C2, C3, or C4 of fucopyranose units are a characteristic feature of fucoidans. Variations may occur in monomer sequences, sulfate substitution patterns, and molecular size of the polymer chains. These structural alterations, which are influenced by environmental factors, were identified in several species of brown algae.

Sargassum natans is considered as an invasive species that affect coastal biodiversity and livelihood of many coastal residents. Eventual decomposition of *S. natans* massive biomass results in a foul smell. Mohammed et al. report the optimization and purification of Sodium alginate from *S. natans* [15]. Large biomass of *S. natans* found in coastal areas of Sri Lanka remains underutilized. It could be a potential candidate for refining alginate, fucoidan, and other natural products.

The current study was part of a project exploring bioactive functionalities of under-explored marine algae inhabiting the Laccadive Sea, bordering Sri Lanka, India, and the Maldives. The objectives were to explore the hypotheses, antioxidant, and cytoprotective potential of fucoidan extracted from *S. natans* against Chinese fine dust (CFD)-induced oxidative stress and apoptosis in HaCaT cells.

2. Materials and methods

2.1. Materials

Urban aerosols (CRM No. 28) designated as CFD was purchased from the National Institute for Environmental Studies, Ibaraki, Japan. The fucoidan standard, 2′ 7′-dichlorodihydrofluorescein diacetate (DCFH2-DA), propidium iodide, Folin-Ciocalteu regent, 3-(4,5-dimethylthiazol-2-yl)-2,5-diphenyltetrazolium bromide (MTT), nitric acid, agarose (low melting point), and deuterated water were purchased from Sigma-Aldrich Corp., St. Louis, MO, USA. HaCaT keratinocytes were purchased from the Korean Cell Line Bank (Seoul, Republic of Korea). Fetal bovine serum (FBS), Dulbecco's Modified Eagle's Medium (DMEM), and antibiotics (penicillin and streptomycin) were procured from Thermo Fisher Scientific, Waltham, MA, USA. Antibodies were obtained from Santa Cruz Biotechnology, Dallas, TX, USA. Organic solvents were of the highest purity grade.

2.2. Algae collection, extraction, and purification of fucoidans

S. natans samples were collected from Hikkaduwa, Sri Lanka. Samples were thoroughly washed, lyophilized, and ground to a powder. The dry powder was first depigmented using 95% ethanol and suspended in an ethanol solution containing 10% formaldehyde for 8 h at 37 °C. The solution was filtered off, and the powder was washed thrice with ethanol. The dry powder was then suspended in sterilized distilled water, and the pH was adjusted to 4.5 using HCl. Then Celluclast was introduced to the suspension at a 0.5% substrate concentration. The digestion was carried out for 24 h at 50 °C with continuous agitation. The extract was recovered by initial coarse filtration using a stainless steel sieve followed by centrifugation at 6000 ×*g*. Celluclast in the filtrate was heat-inactivated by incubating in a boiling water bath for 10 min. The mixture was then adjusted to a pH of 8.0 by NaOH. Then Alcalase was incorporated at 0.1% of substrate weight and incubated for 8 h at 50 °C under continuous agitation. Alcalase was heat-inactivated, and the pH was adjusted to 4.0 using HCl. A saturated solution of $CaCl_2$ was gradually incorporated into the mixture to precipitate alginate. After centrifugation, the pH of the supernatant was adjusted to 7.0 by NaOH. The volume of the mixture was reduced to 1/4th of its initial extraction volume via lyophilization. Then, four volumes of 95% ethanol were incorporated to the mixture to precipitate the polysaccharides. The precipitated polysaccharides were washed with ethanol, dissolved in DW, and dialyzed. Precipitated polysaccharides were further fractionated by a DEAE-sepharose anion exchange open column. The column was equilibrated with sodium acetate buffer (50.0 mM, pH 5.3), The sample was loaded and eluted with 200 ml of each solvent system with increasing concentrations of NaCl in the same buffer (0, 0.2, 0.4, 0.6, 0.8, 1.0, 1.2, 1.4, 1.6, 1.8, and 2.0). The eluents were collected by a Gilson FC 203B fraction collector (Villiers Le Bel, France) into conical tubes (10 ml each), and the polysaccharide contents in tubes were measured by phenol-sulfuric assay [16]. The tubes were pooled into 7 fractions (SNF1 – SNF7) based on their polysaccharide contents.

2.3. Analysis of the chemical composition

Polysaccharide, polyphenol, and protein levels were analyzed respectively by phenol-sulfuric assay, Folin-Ciocalteu method, and using a BSA protein assay kit [16,17]. Sulfate content was analyzed by the $BaSO_4$ precipitation method [18]. For the analysis of monosaccharide composition, a portion of the fractions was hydrolyzed using trifluoroacetic acid and analyzed after resolving in a CarboPac PA1 cartridge column integrated to an ED50Dionex electrochemical detector.

2.4. FTIR, NMR, and molecular weight (MW) distribution analysis

FTIR spectra were taken using NicoletTM 6700 FTIR spectrometer, Thermo Scientific, MA, USA, by KBr pelleting method. NMR analysis was done following the deuterium exchange. The polysaccharide sample was dissolved in D_2O, and a minute amount of methanol was incorporated as the internal standard. The analysis was done at 33 k using a JNMECX400, NMR spectrometer, JEOL, Japan. The MW distribution pattern of the polysaccharide fractions was analyzed by agarose gel electrophoresis using dextran sulfate and chondroitin sulfate MW markers [19].

2.5. Cell culture; evaluating the protective effects of SNF against CFD-induced oxidative stress

HaCaT keratinocytes were cultured and maintained in DMEM media supplemented with 1% penicillin/streptomycin mixture and 10% FBS. Cultures were maintained in a humidified atmosphere under 37 °C supplemented with 5% CO_2. Exponentially replicating cells were seeded for experiments at a 1×10^5 cells mL^{-1} concentration. After 24 h, different concentrations of the column fractions were treated into the cells and again after 1 h, stimulated with 125 μg mL^{-1} of CFD. The final concentration of CFD (125 μg mL^{-1}) was optimized based on preliminary experiments on cell viability and intracellular ROS levels [20]. After a 30 min incubation period, the wells were washed twice by PBS to remove CFD, and new culture media was added. After 1 h, intracellular ROS levels were determined by DCFH2-DA assay, and after 24 h, cell viability was measured by MTT assay [21]. For the selected sample SNF7, the treated cells were stained with DCFH2-DA for fluorescence microscopy (CoolSNAP-Pro color digital camera) and flow cytometry analysis following our previously described methods [20].

2.6. ICP-OES analysis

The treatment and stimulation of cells followed the same method as described above. The cells were harvested washed in PBS by resuspension and transferred to dry preweighted vials. The cells were dried in

Please cite this article as: I.P.S. Fernando, K.K.A. Sanjeewa, H.G. Lee, et al., Characterization and cytoprotective properties of *Sargassum natans* fucoidan against urban aerosol-induced keratinocyte damage..., , https://doi.org/10.1016/j.ijbiomac.2020.05.132

a drying oven at 105 °C overnight. The dried cells were digested in conc. Nitric acid containing 30% H_2O_2 for 30 min at 105 °C. The digests were diluted in ultrapure DW (Milli-Q® IntegralWater Purification System, MilliporeSigma, Burlington, MA, USA) containing 3% HNO_3. Metal ions were analyzed by an inductively coupled plasma optical emission spectrometry (ICP-OES) (OPTIMA 7300DV, PerkinElmer, Inc., Waltham, MA, USA). The spectrometer was calibrated with a multi-element standard (PerkinElmerN9300233).

2.7. Evaluation of CFD-induced apoptotic body formation

Following the above mentioned sample treatment and CFD-stimulation, HaCaT cells were stained with Hoechst 33342 (10 μg mL^{-1}) or a mixture of acridine orange/ethidium bromide (100 μg mL^{-1}) [22]. After a 10 min incubation, fluorescence images of the cells were taken by a fluorescence microscope, integrated to a CoolSNAP-Pro color digital camera.

2.8. Cell cycle analysis

Flow cytometry analysis of the cell cycle was carried out to determine the cells residing in the sub-G_1 phase of the cell cycle following the method by [22]. The analysis was done using a Becton Dickinson FACSCalibur flow cytometer (San Jose, CA, USA). The pre-seeded cells were treated with different sample concentrations and stimulated with CFD. After 24 h, the cells were harvested and kept fixed in 70% ethanol. For the analysis, the cells were first washed with PBS containing 2 mM of EDTA and mixed with a solution containing RNase and the PI stain.

2.9. Comet assay

Protective effects of the sample against the CFD-induced DNA damage were evaluated by comet assay following the method by [22]. Briefly, the pre-seeded cells were treated with different sample concentrations and stimulated with CFD. After 24 h, the cells were harvested and used for the comet assay analysis.

2.10. Western blot analysis

Western blot analysis was done following the method by Fernando et al. [22]. The cells were harvested and lysed using NE-PER® Nuclear and Cytoplasmic extraction kit (Thermo Scientific, Rockford, USA). The lysates were quantified for their protein levels using a Pierce™ BCA Protein Assay Kit (Thermo Scientific, Rockford, USA). Proteins (40 μg) were loaded to 12% SDS-polyacrylamide gels, and electrophoresis was carried out at 100 V. The bands were visualized by doping with an enhanced chemiluminescence reagent (Amersham, Arlington Heights, IL, USA) and visualized by a Fusion Solo Vilber Lourmat system (Paris, France).

2.11. Statistical analysis

All data values are indicated as means ± SD based on at least three independent evaluations. Significant differences among the data values were calculated using IBM SPSS Statistics 20 software by Duncan's multiple range test using one-way ANOVA. ** P-values <0.05 ($P < 0.05$) were considered significant.

3. Results

3.1. Yield and composition of general components

S. natans raw material contained 62.44 ± 0.52% carbohydrates, 17.22 ± 0.06% ash, 10.35 ± 0.55% proteins, and 1.62 ± 0.05% lipids by dry weight. The ethanol precipitate (SNF) gave a 5.25% yield from the initial sample dry weight and indicated a polysaccharide content of 67.92 ± 0.58% with a 26.42 ± 0.36% sulfate content. The protein and polyphenol contents in SNF were 1.92 ± 0.05% and 4.50%, respectively.

3.2. Fractionation of polysaccharides by anion exchange chromatography

SNF was separated into seven fractions based on polysaccharide ionic charge by DEAE-sepharose anion exchange chromatography (Fig. 1A). We identified seven prominent peaks based on the polysaccharide content analysis. The three minor peaks at tube numbers range 73–84, 153–158, and 173–177 were not studied due to their low yield, which was insufficient for carrying out further analysis. Fourier-transform infrared spectroscopy (FTIR) spectra (Fig. 1B) indicated peaks corresponding to different functional groups. The peak at 845 cm^{-1} is attributable to the bending vibration of C-O-S. An asymmetric carboxylate O-C-O vibration is indicated by 1616 cm^{-1} peak. The broad peak centered at 1035 cm^{-1} represent stretching vibrations of a glycosidic bond, which is common to all polysaccharides and hence could be considered as a reference peak. The prominent peak between 1220 and 1270 cm^{-1} indicate stretching vibrations of S═O bonds in sulfate groups [19,23]. The relative intensity increment of 1220–1270 cm^{-1} peak (sulfate groups) in comparison to reference peak at 1035 cm^{-1} indicate the increase of sulfate group substitutions in subsequent fractions. SNF7 showed the most prominent 1220–1270 cm^{-1} peak, which corresponds to its higher degree of sulfation.

3.3. Characterization of polysaccharide fractions

Table 1 indicates the composition of the general components in each of the column fractions. Polysaccharides were the main components in all fractions. The monosaccharide composition of each polysaccharide fraction was analyzed after hydrolysis with trifluoroacetic acid. The polysaccharide content and sulfate content showed a reciprocal variation in successive fractions, while the polysaccharide content gradually decreased, the sulfate content gradually increased. SNF7 had the highest sulfate content (36.41 ± 0.59%). There was no exact pattern in the protein and polyphenol contents. The major monosaccharide component in all fractions was fucose, which gradually increased in successive fractions.

The MW distributions of the fractions were approximated by agarose gel electrophoresis (Fig. 2A) in comparison to known sulfated polysaccharide molecular weight (MW) standards. The MW distributions gradually decreased with each subsequent fraction. The mean value of MW distributions of fractions SNF1-SNF7 was respectivelly approximated as 135, 120, 110, 95, 90, 85, and 50 kDa. Based on ^{1}H NMR chemical shifts shown in Fig. 2B, signals in between 0.95 and 1.35 ppm can be assigned to methyl protons of fucopyranose units [24]. As described by [25], chemical shifts of anomeric protons can be used to designate between α- and β- anomers. Anomeric protons of α-fucose reside within 5.10–5.40 ppm, whereas peaks for protons H2 - H4 resided within the 3.5–4.5 ppm region [26]. The noise level was higher in the ^{13}C spectrum (Fig. 2C), probably due to the high polydispersity index of these polymers. However, certain peaks could be identified, such as the peaks at 12.5–17.5 ppm, which represented C6 methyl groups. Peaks between 95.0 and 105.0 ppm may contain peaks for C1 carbon atoms, whereas the peak range 65–75 ppm may contain peaks representing ring carbon atoms (C2-C5) [26].

3.4. Protective effects of polysaccharide fractions against CFD-induced oxidative damage

As shown in Fig. 3A, none of the fractions within the examined concentration range are cytotoxic on HaCaT cells. Hence a 12.5–100 μg mL^{-1} concentration range was considered safe for further experiments. According to Fig. 3B, CFD treatment causes a prominent increase in intracellular ROS levels and a decrease in HaCaT cell viability.

Please cite this article as: I.P.S. Fernando, K.K.A. Sanjeewa, H.G. Lee, et al., Characterization and cytoprotective properties of *Sargassum natans* fucoidan against urban aerosol-induced keratinocyte damage..., , https://doi.org/10.1016/j.ijbiomac.2020.05.132

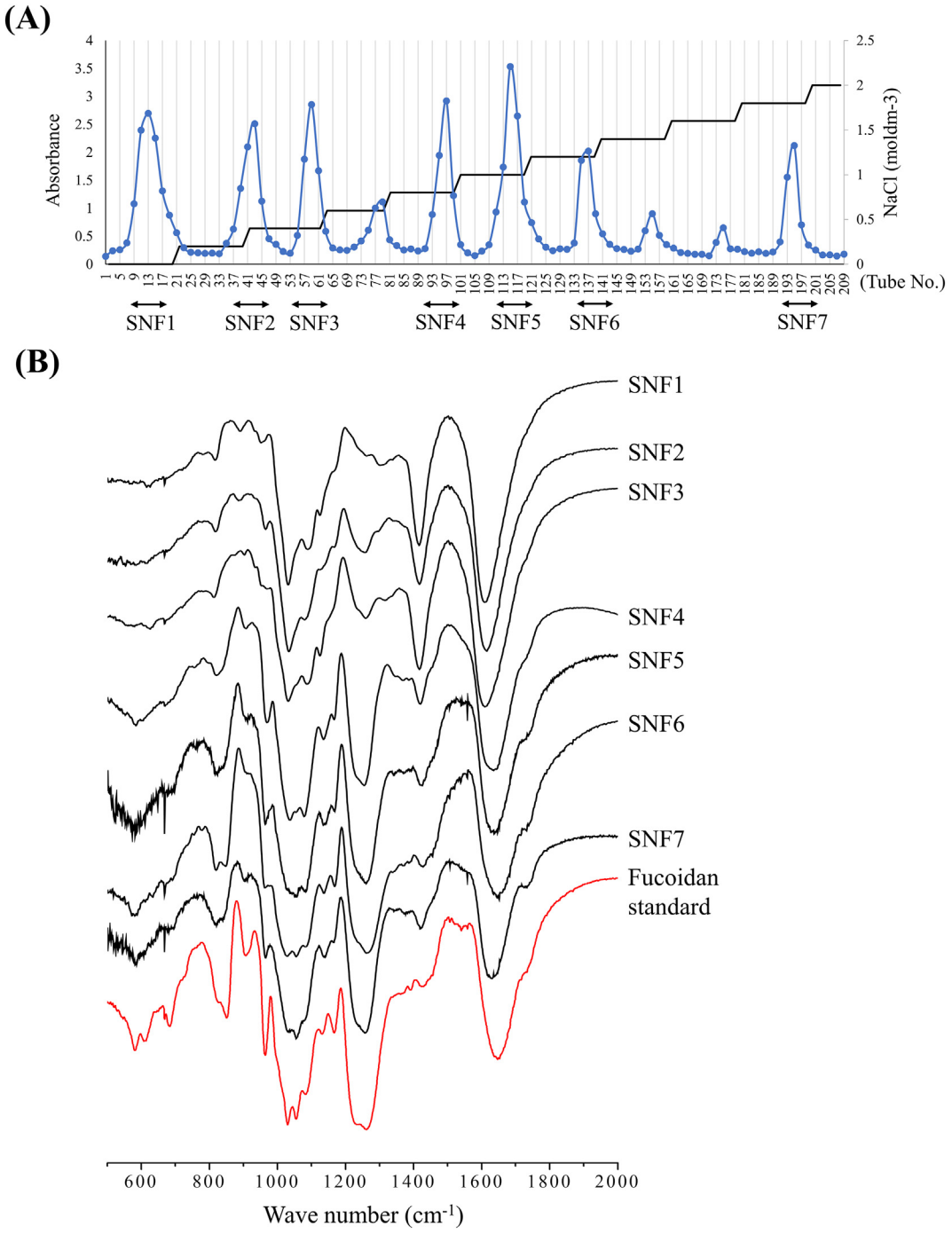

Fig. 1. Fractionation of crude polysaccharides. (A) Anion exchange chromatography purification of crude polysaccharides. (B) FTIR analysis of purified fractions (SNF1-SNF7).

Treatment of polysaccharide fractions dose-dependently reduced the CFD-induced ROS levels and increased cell viability. A trend was observed, where the antioxidant activity and cytoprotective effects increased in successive fractions. SNF7 showed the best antioxidant activity among all fractions with an IC_{50} of 22.45 ± 2.73 μg mL^{-1}. The inhibitory effects of SNF7 on intracellular ROS generation were further confirmed by DCFH2-DA staining by both fluorescence microscopy (Fig. 3C) and flow cytometry (Fig. 3D). Per the fluorescence images, the green color intensity was dose-dependently reduced with SNF7 staining compared to the CFD-stimulated cells. Per FACS analysis, a peak shift to higher intensity (FITC axis) denoted increased ROS levels. The treatment of SNF7 dose-dependently lowered the cell population, which had a higher ROS level. The gating strategy used during the FACS analysis excludes fluorescence of cellular debris and only considered the cell count based on the fluorescence intensity of viable cells.

3.5. SNF7 could chelate metal ions in CFD-treated HaCaT keratinocytes

Treatment of CFD increased the metal ions, Pb, Sr, Ca, Ba, Fe, Al, Mg, As, Cu, and Cr in HaCaT cells (Table 2), compared to the control. SNF7 dose-dependently reduced the content of a particular set of metal ions, including Pb > Fe > Ca > Sr > Ba and Mg.

Please cite this article as: I.P.S. Fernando, K.K.A. Sanjeewa, H.G. Lee, et al., Characterization and cytoprotective properties of *Sargassum natans* fucoidan against urban aerosol-induced keratinocyte damage..., , https://doi.org/10.1016/j.ijbiomac.2020.05.132

Table 1
The composition of column fractions.

		SNF1	SNF2	SNF3	SNF4	SNF5	SNF6	SNF7
Yield (%)		16.55 ± 0.66	14.23 ± 0.13	12.20 ± 0.07	12.48 ± 0.94	17.28 ± 0.58	11.02 ± 0.27	8.13 ± 0.76
Chemical composition (%)	Polysaccharide	82.32 ± 0.12	77.35 ± 0.42	74.72 ± 0.08	69.73 ± 0.55	66.41 ± 0.35	63.33 ± 0.05	54.25 ± 0.55
	Sulfate	8.34 ± 0.94	12.96 ± 0.92	15.81 ± 0.89	20.85 ± 0.84	24.07 ± 0.49	27.30 ± 0.24	36.41 ± 0.59
	Protein	0.21 ± 0.01	0.20 ± 0.02	0.23 ± 0.01	0.21 ± 0.01	0.19 ± 0.00	0.20 ± 0.02	0.22 ± 0.03
	Polyphenol	0.53 ± 0.02	0.53 ± 0.01	0.52 ± 0.02	0.44 ± 0.04	0.47 ± 0.02	0.42 ± 0.02	0.4 ± 0.02
Monosaccharide composition (%)	Fucose	45.70	45.85	51.92	53.32	59.74	61.65	70.97
	Rhamnose	0.26	0.36	0.67	0.65	1.36	1.82	1.015
	Galactose	28.01	26.65	20.43	18.59	15.54	10.97	6.77
	Glucose	3.12	2.61	2.53	1.95	1.85	1.38	0.53
	Xylose	19.11	19.23	10.91	11.31	9.33	5.66	2.39
	Others	3.79	5.31	13.56	14.19	12.18	18.51	18.31

3.6. SNF7 reduced the formation of apoptotic bodies in CFD treated HaCaT cells

The CFD treatment induced the formation of apoptotic bodies in HaCaT cells, as seen from the Hoechst 33342 stain (Fig. 4A). Also, a considerable proportion of the cells were identified to be in late apoptosis based on the nuclear double staining with acridine orange and ethidium bromide (Fig. 4B). The appearance of fragmented green and orange color nuclear morphology indicates cells in late apoptosis. These events could be revoked by dosing with SNF7. Cell cycle analysis indicated paranal results, whereas SNF7 lowered sub-G_1 apoptotic cell populations, which was augmented upon CFD treatment (Fig. 4C).

3.7. SNF7 reduced the CFD-induced DNA damage in HaCaT keratinocytes

As evident from the comet assay (Fig. 5A), CFD treatment caused DNA damage, as seen from the increased tailing smear of the comet compared to the control. The damage was reduced dose-dependently upon the application of SNF7. Western blot analysis was carried out to identify the levels of crucial apoptosis regulatory proteins, which might mediate CFD-induced apoptosis. As shown in Fig. 5B, CFD enhances the levels of Bax, caspase-3, caspase-9, and cleavage of poly (ADP-ribose) polymerase (PARP) while decreasing Bcl-xL levels. As shown in Fig. 5C and D, CFD-stimulation increases the levels of antioxidant enzymes, including superoxide dismutase (SOD), catalase (CAT), and heme oxygenase (HO-1) in the cytoplasm and nuclear factor erythroid 2-related factor 2 (NRF2) in the nucleus of the HaCaT keratinocytes. Treatment with SNF7 further increased their levels, enhancing the protective effects against CFD-induced oxidative stress.

4. Discussion

The present purification approach using Celluclast gives a higher fucoidan yield compared to conventional water extracts [19]. Further, the acidic pH conditions optimal to Celluclast activity minimized the contamination of the extract with alginate. Polymerizing polyphenols, with the addition of formaldehyde, prevented the contamination of polysaccharides with polyphenols. Alcalase hydrolyzes proteins into small peptides and amino acids, thereby increasing their solubility, which in turn minimizes their precipitation during the addition of ethanol [19]. The chemical composition of the ethanol precipitate indicated a polysaccharide content of 67.92 ± 0.58% with a 26.42 ± 0.36% sulfate content. The negligible levels of protein and polyphenol contents confirmed the effectiveness of this extraction method for enriching fucoidans.

Anion exchange chromatographic purification fractionated the crude polysaccharides into seven sensible fractions. We observed the elution of fractions for each mobile phase solvent system having different NaCl concentrations. However, the yield of some fractions (three of

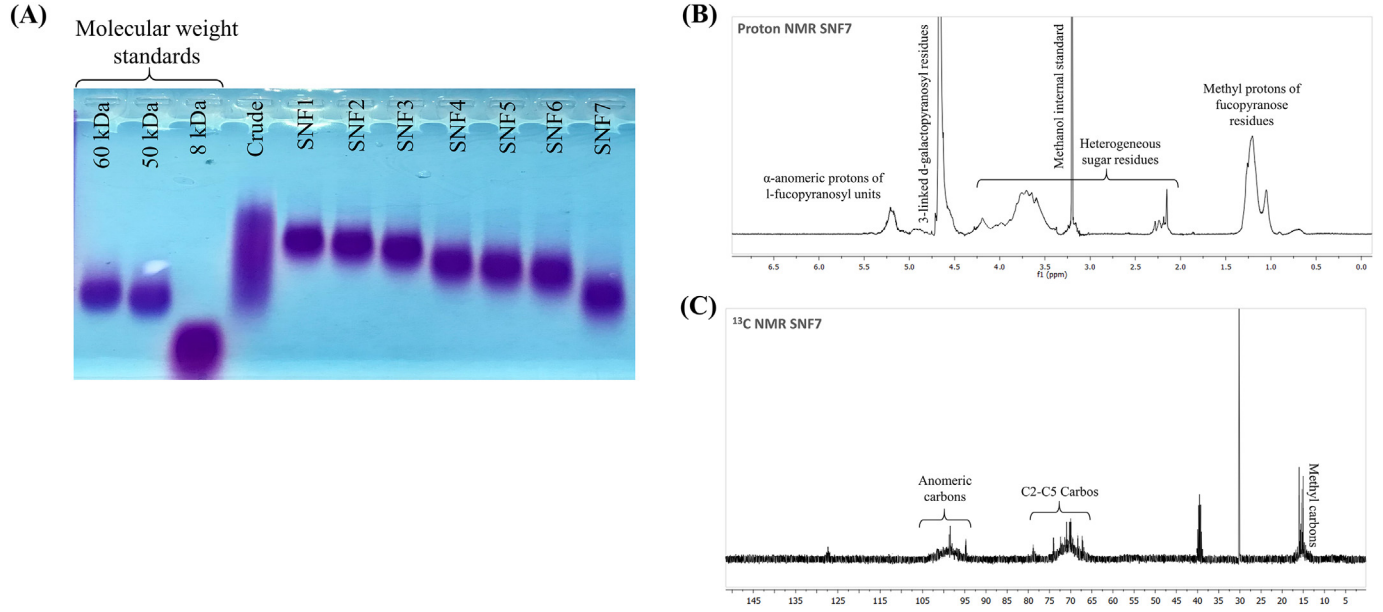

Fig. 2. Polysaccharide characterization. (A) Molecular weights of polysaccharide fractions after column separation as analyzed by agarose gel electrophoresis. Characterization of SNF7 (B) ^{1}H NMR, and (C) ^{13}C NMR.

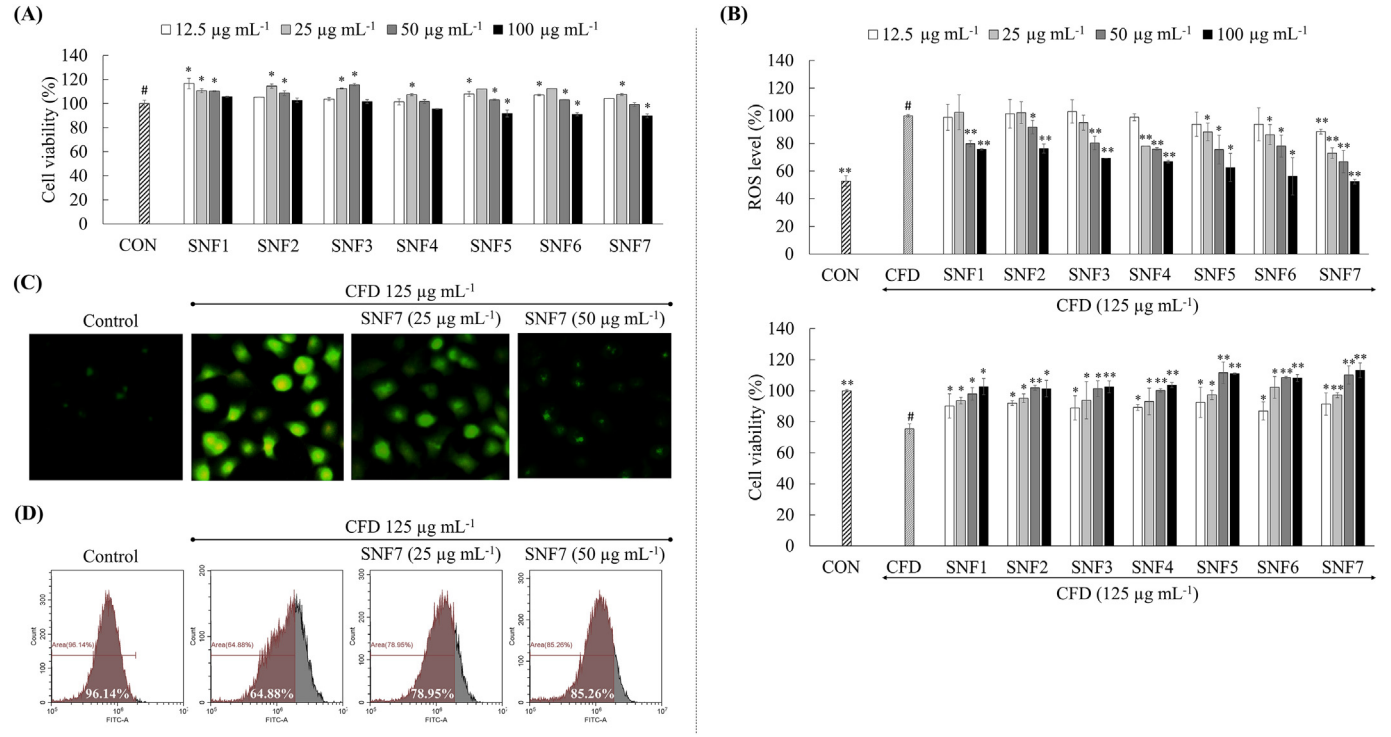

Fig. 3. Cytotoxicity and protective effects of polysaccharide fractions against the CFD induced oxidative damage. (A) Cytotoxicity of polysaccharide fractions in HaCaT keratinocytes, (B) Effects of polysaccharide fractions on CFD induced ROS levels, and cell viability. Effects of SNF7 on CFD induced ROS levels as evaluated by (C) fluorescence microscopy and (D) flow cytometry. Cell viability was evaluated by MTT assay, and DCFH2-DA stain was used to measure ROS levels by fluorescence microscopy and flow cytometry. The results are means ± SD ($n = 3$). Significant difference "#" from control (A) and CFD alone (B) were considered as $^{*}P < 0.05$ and $^{**}P < 0.01$.

them) was too low for further studies. The polysaccharide and sulfate contents in each successive fraction indicated a counter-parallel relationship, where the polysaccharide content decreased while the sulfate content was elevated, increasing its anionic characteristics. The anion exchange chromatographic systems are designed to elute the most negatively charged molecules last [19]. The increasing sulfate content in successive fractions was explained by the above scenario. The monosaccharide composition of the fractions indicated an increase in the fucose content in successive fractions. Trifluoroacetic acid supposedly hydrolyzes the polymer, while desulfating it giving monosaccharides. However, observation of a few spurious peaks in all HPAEC-PAD chromatograms suggests a minor flaw in the desulfation of fucose units. Considering the high abundance of fucose, we neglected the above error and reported them under the term "others" in the Table 1. As defined earlier, fucoidan is a fucose-rich sulfated polysaccharide. The ion-exchange chromatography led to the purification of fucoidans, and the ideal fucoidan features increased with successive fractions.

FTIR spectrum of SNF7 indicated a higher degree of similarity to the fucoidan standard. The prominent peak between 1220 and 1270 cm^{-1} agreed with its higher sulfate substitution compared with other fractions. The active fraction, SNF7, was characterized by NMR analysis, which showed characteristic peaks of fucoidan as described in the results section.

Treatment of each fraction dose-dependently reduced the intracellular ROS levels in CFD-induced HaCaT keratinocytes. SNF7 showed the most prominent activity. Simultaneously, an increase in the cell viability was observed for each fraction, indicating cytoprotective effects against CFD-induced oxidative stress. The antioxidant molecular mechanism of SNF7 was investigated by analyzing levels of some key antioxidant enzymes. Fucoidans are known to promote cellular antioxidant defense

Table 2
Metal ion composition in cells (ppm).

Element	Control	CFD	CFD + SNF7 (25 μg mL^{-1})	CFD + SNF7 (50 μg mL^{-1})	CFD + SNF7 (100 μg mL^{-1})
Na	717 ± 6	724 ± 7	728 ± 11	718 ± 17	723 ± 14
Mg	116 ± 21**	178 ± 7	155 ± 18	149 ± 22	119 ± 12**
Al	ND	84 ± 2	81 ± 24	73 ± 7	62 ± 8*
K	475 ± 10	477 ± 11	468 ± 17	463 ± 13	473 ± 6
Ca	169 ± 20**	456 ± 6	429 ± 16	404 ± 4**	307 ± 11**
Fe	67 ± 11**	274 ± 12	259 ± 13	195 ± 22**	117 ± 11**
Mn	ND	68 ± 7	67 ± 12	62 ± 7	46 ± 12
Cu	ND	26 ± 5	22 ± 2	16 ± 4	11 ± 4*
As	ND	41 ± 12	39 ± 13	35 ± 0	28 ± 6
Sr	8 ± 6**	176 ± 16	165 ± 18	141 ± 16	101 ± 17**
Ba	ND	113 ± 11	79 ± 4**	69 ± 9**	43 ± 16**
Pb	ND	369 ± 19	323 ± 17*	268 ± 18**	150 ± 5**
Cr	ND	26 ± 11	25 ± 6	21 ± 8	23 ± 4

All metal ion concentrations are given in parts per million (ppm). N.D. stands for not detected. CFD concentration was 125 μg mL-1. Results were obtained by triplicate determinations ($n = 3$) and presented as means ± SD. * $P < 0.05$ and ** $P < 0.01$ were considered significant compared to the CFD (only) treated group.

Please cite this article as: I.P.S. Fernando, K.K.A. Sanjeewa, H.G. Lee, et al., Characterization and cytoprotective properties of *Sargassum natans* fucoidan against urban aerosol-induced keratinocyte damage..., , https://doi.org/10.1016/j.ijbiomac.2020.05.132

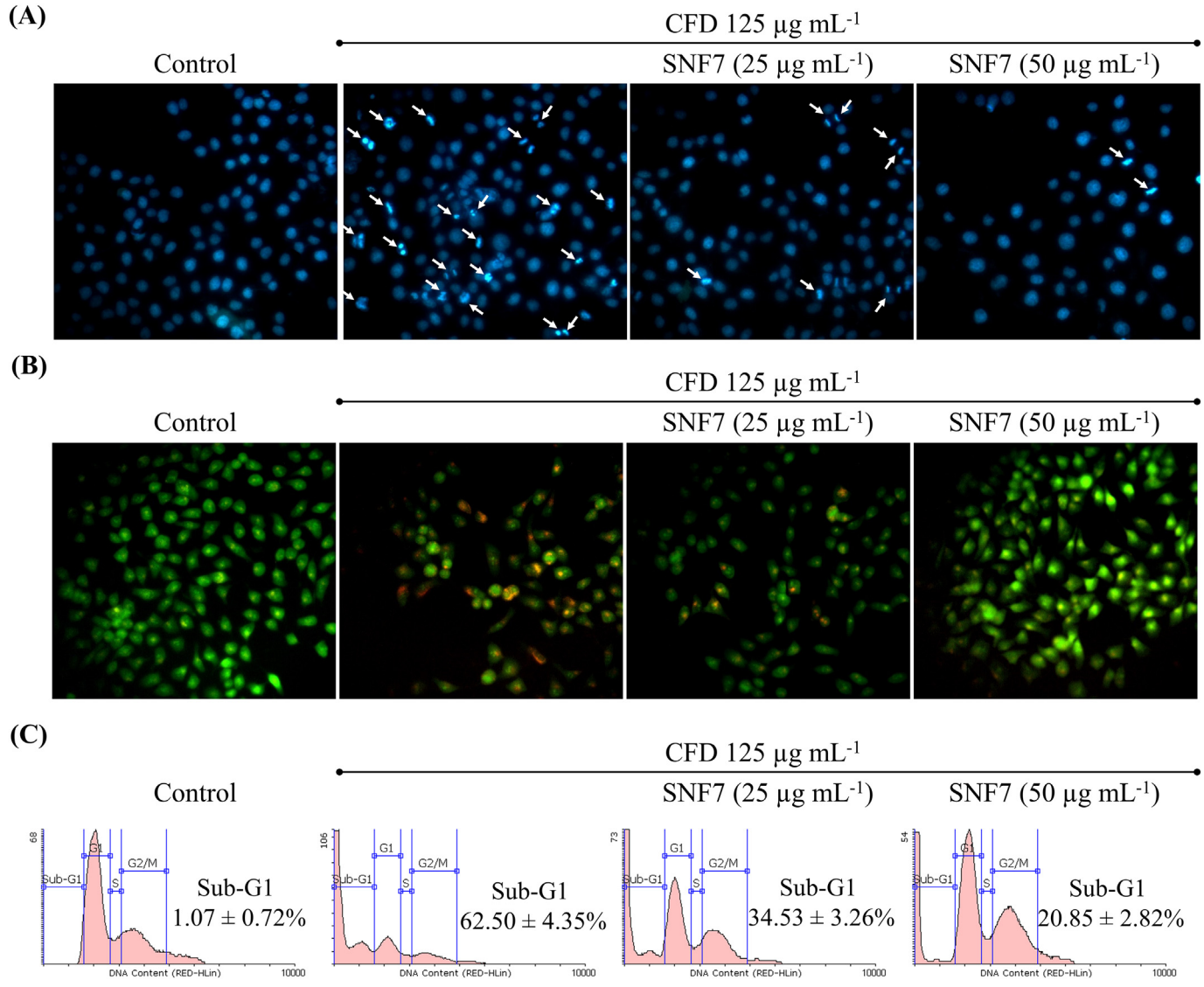

Fig. 4. Effect of SNF7 on CFD induced apoptosis in HaCaT keratinocytes. Evaluation of apoptotic body formation by fluorescent staining using (A) Hoechst 33342 and (B) double staining using acridine orange and ethidium bromide. (C) Cell cycle analysis of sub-G_1 populations of hyperdiploid cells. Repeatability of results was confirmed by triplicate determinations (n = 3) and presented as means ± SD.

by increasing the levels of antioxidant enzymes such as HO-1, SOD, and CAT [27]. The western blot analysis revealed that SNF7 could dose-dependently augment HO-1, SOD, and CAT levels in CFD-induced HaCaT keratinocytes. Nrf2 is an important transcription factor that regulates the expression of antioxidant genes such as HO-1, CAT, and SOD by binding to antioxidant response elements. The up-regulation of these enzymes via Nrf2 transcription increases the cytoprotective responses and plays an essential role in attenuating oxidative stress [28].

CFD used in the present study consists of mainly 14.9% of Si, 12% of C, 6.69% of Ca, 5.04% of Al, 3.91% of S, 2.92% of Fe, 1.40% of Mg, 1.37% of K, 0.807% of Cl, 0.796% of Na, 0.79% of N, 0.292% of Ti, 0.145% of P and 0.144% of Zn with other elements found at minor level. Other than inorganic constituents CFD contain polycyclic aromatic hydrocarbons (PAH) including pyrene, indeno (1,3,3,-cd) pyrene, fluoranthene, benzo (b) fluoranthene, benzo (ghi) perylene, benz (a) anthracene, benzo (a) pyrene and benzo (k) fluoranthene [29]. Previously, it has been shown that fucoidan can act as a chelating agent, which indicates affinity towards divalent metal ions such as Pb^{2+}, Ba^{2+}, Cd^{2+}, Sr^{2+}, Cu^{2+}, Fe^{2+}, Mg^{2+} and Ca^{2+} [30]. Our previous findings involving GC–MS/MS analysis indicated that PAH in CFD doesn't have a significant effect on keratinocyte viability and ROS production [31]. The damaging effects were mainly attributed to heavy metals sourcing from CFD. Inductively coupled plasma-optical emission spectrometry evaluations indicated that SNF7 could dose-dependently reduce the content of some metal ions such as Pb^{2+}, Ba^{2+}, Sr^{2+}, Cu^{2+}, Fe^{2+}, and Ca^{2+} in HaCaT keratinocytes. Alginate over fucoidan is renowned as a prominent metal ion chelator [31]. Fewer studies describe the metal ion chelation effects of fucoidans [30]. The ability of SNF7 to reduce toxic metal ions could have a positive effect on the observed cytoprotective results.

A cytotoxic material could impose cell death through apoptosis or necrosis. Apoptosis is a genetically controlled approach of cell death characterized by cell shrinkage, DNA fragmentation, and membrane blebbing [32]. The DNA damage is a key biological marker for evaluating oxidative stress-induced apoptosis [33]. CFD treatment causes the formation of apoptotic bodies, as seen from the fluorescence image analysis in Fig. 4A and B. Also, the cell-cycle analysis revealed the accumulation of cells in the sub-G_1 phase, which was indicative of apoptosis. Additionally, SNF7 treatment reduced the apoptotic cells dose-dependently, exhibiting its cytoprotective effects. A comet assay is another versatile and sensitive approach to analyze DNA damage [22]. The tail DNA percentage abruptly increased upon CFD treatment for a 24 h period. A dramatic dose-dependent decrease was observed upon

Please cite this article as: I.P.S. Fernando, K.K.A. Sanjeewa, H.G. Lee, et al., Characterization and cytoprotective properties of *Sargassum natans* fucoidan against urban aerosol-induced keratinocyte damage..., , https://doi.org/10.1016/j.ijbiomac.2020.05.132

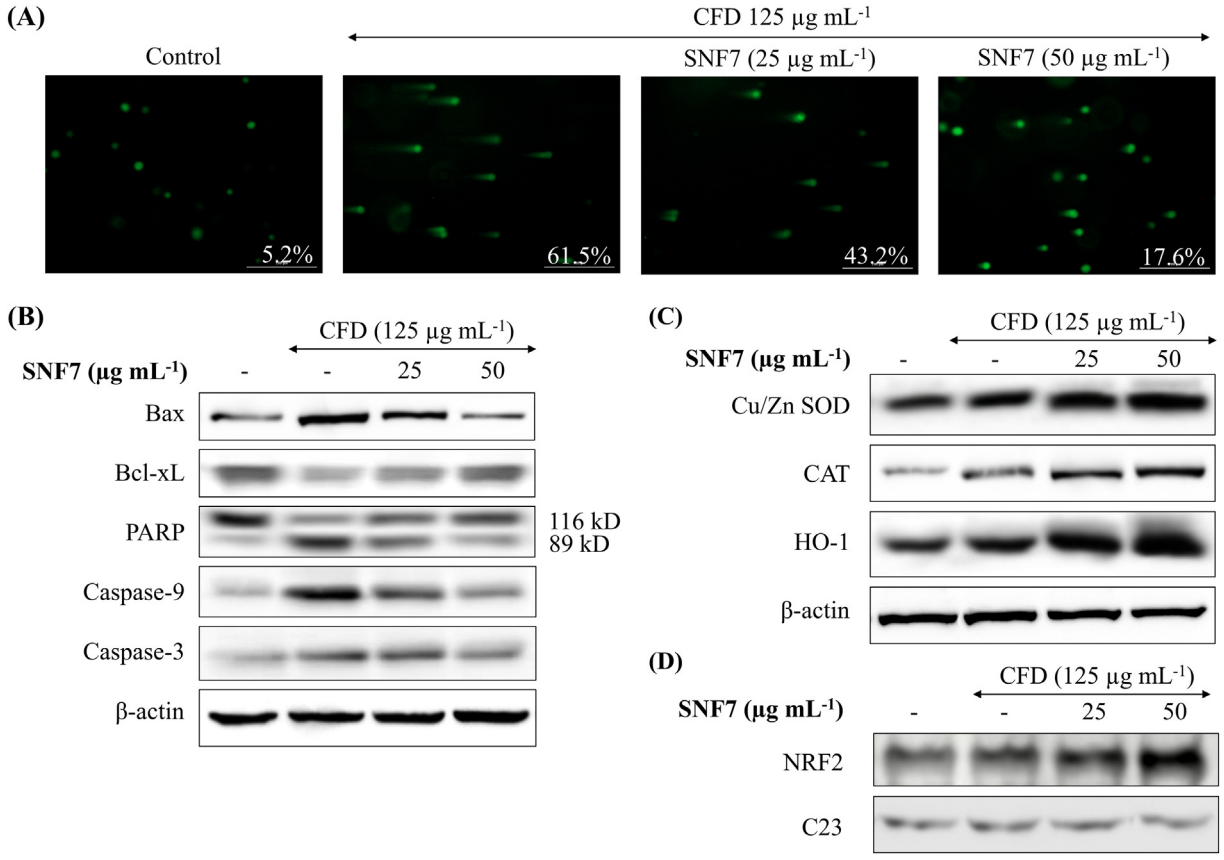

Fig. 5. Effect of SNF7 on CFD induced DNA damage and mediation of apoptosis in HaCaT keratinocytes. (A) Effect on DNA damage as assessed by comet assay. (B) Effects on apoptosis-related key molecular mediators. Effects on levels of antioxidant enzymes in (C) cytosol and (D) nucleus. Repeatability of results was confirmed by triplicate determinations (n = 3).

SNF7 treatment. These results suggested that SNF7 could protect the cells against CFD-induced damage.

Apoptosis is a process mediated by a complex system of cell-signaling pathways. Mitochondria are the main target in oxidative stress-induced apoptosis [28]. Cytochrome c released from mitochondria can activate caspase-9, an initiator caspase that gets triggered by apoptosomes [34]. Activated caspase-9 activates downstream caspases such as caspase-3, -6, and -7, which initiate signaling pathways leading to cell death. Other than this, pro and anti-apoptotic proteins come into play, whereas Bax mediates the release of cytochrome *c* and pro-apoptotic factors from mitochondria [35]. Alternatively, the anti-apoptotic protein, Bcl-xL, works the other way by competitively inhibiting Bax by binding to tBid, which activates Bax. Activation of Bcl-xL while inhibiting Bax is, therefore, a desirable property for achieving cytoprotective effects. Hence, the reduction of the Bax/Bcl-xL ratio is considered to be an important prognostic factor of cytoprotectivity, which agrees with the present observations. Cleavage of PARP, which maintains DNA stability and regulates DNA repair and transcription is another characteristic feature seen during apoptosis [36]. The present evidence collectively indicated that CFD could induce apoptosis in HaCaT keratinocytes via the mitochondria-mediated intrinsic pathway, whereas SNF7 could dose-dependently increase cytoprotective effects.

With fine dust air pollution increasing in many parts of the world, the need for pharmaceutical agents that could counter the detrimental effects of PM has become a timely requirement. In conclusion, the fucoidan-rich SNF7 fraction showed promising cytoprotective effects in HaCaT keratinocytes against urban PM-induced oxidative stress by boosting antioxidant defense mechanisms. These fucoidans showed great potential to be developed into cosmeceuticals to counter the detrimental effects of PM exposure to skin. Although some rocky coastal areas of Sri Lanka flourish with algae, none of them are utilized and remain idle. These underutilized algal bioresources could be used in industry for manufacturing safe and efficient consumables.

Declarations of competing interest

None.

CRediT authorship contribution statement

Ilekuttige Priyan Shanura Fernando: Conceptualization, Methodology, Investigation, Validation, Formal analysis, Writing - original draft. **Kalu Kapuge Asanka Sanjeewa:**Methodology, Investigation, Validation.**Hyo Geun Lee:**Methodology, Investigation, Validation.**Hyun-Soo Kim:**Formal analysis, Data curation.**Andaravaas Patabadige Jude Prasanna Vaas:**Formal analysis, Data curation.**Hondamuni Ireshika Chathurani De Silva:**Formal analysis, Supervision.**Chandrika Malkanthi Nanayakkara:**Formal analysis, Supervision.**Dampegamage Thusitha Udayangani Abeytunga:**Project administration, Supervision. **Won Woo Lee:**Project administration, Formal analysis, Data curation. **Dae-Sung Lee:**Resources, Project administration, Funding acquisition. **You-Jin Jeon:**Resources, Writing - review & editing, Supervision, Project administration, Funding acquisition.

Acknowledgments

This research was supported by a grant from the Marine Biotechnology Program (20170488) funded by the Ministry of Oceans and Fisheries, Korea.

Please cite this article as: I.P.S. Fernando, K.K.A. Sanjeewa, H.G. Lee, et al., Characterization and cytoprotective properties of *Sargassum natans* fucoidan against urban aerosol-induced keratinocyte damage..., , https://doi.org/10.1016/j.ijbiomac.2020.05.132

References

[1] K.E. Kim, D. Cho, H.J. Park, Air pollution and skin diseases: adverse effects of airborne particulate matter on various skin diseases, Life Sci. 152 (2016) 126–134.
[2] J.O. Anderson, J.G. Thundiyil, A. Stolbach, Clearing the air: a review of the effects of particulate matter air pollution on human health, J. Med. Toxicol. 8 (2) (2012) 166–175.
[3] M. Guarnieri, J.R. Balmes, Outdoor air pollution and asthma, Lancet 383 (9928) (2014) 1581–1592.
[4] D. Peden, C.E. Reed, Environmental and occupational allergies, J. Allergy Clin. Immunol. 125 (2, Supplement 2) (2010) S150–S160.
[5] S. Song, K. Lee, Y.-M. Lee, J.-H. Lee, S. Il Lee, S.-D. Yu, D. Paek, Acute health effects of urban fine and ultrafine particles on children with atopic dermatitis, Environ. Res. 111 (3) (2011) 394–399.
[6] G. Tsuji, M. Takahara, H. Uchi, S. Takeuchi, C. Mitoma, Y. Moroi, M. Furue, An environmental contaminant, benzo(a)pyrene, induces oxidative stress-mediated interleukin-8 production in human keratinocytes via the aryl hydrocarbon receptor signaling pathway, J. Dermatol. Sci. 62 (1) (2011) 42–49.
[7] I. Oh, J. Lee, K. Ahn, J. Kim, Y.-M. Kim, C. Sun Sim, Y. Kim, Association between particulate matter concentration and symptoms of atopic dermatitis in children living in an industrial urban area of South Korea, Environ. Res. 160 (2018) 462–468.
[8] K. Ahn, The role of air pollutants in atopic dermatitis, J. Allergy Clin. Immunol. 134 (5) (2014) 993–999.
[9] A. Vierkötter, T. Schikowski, U. Ranft, D. Sugiri, M. Matsui, U. Krämer, J. Krutmann, Airborne particle exposure and extrinsic skin aging, J. Invest. Dermatol. 130 (12) (2010) 2719–2726.
[10] S.P. Yun, S.J. Lee, S.Y. Oh, Y.H. Jung, J.M. Ryu, H.N. Suh, M.O. Kim, K.B. Oh, H.J. Han, Reactive oxygen species induce MMP12-dependent degradation of collagen 5 and fibronectin to promote the motility of human umbilical cord-derived mesenchymal stem cells, Br. J. Pharmacol. 171 (13) (2014) 3283–3297.
[11] M. Nakamura, A. Morita, S. Seité, T. Haarmann-Stemmann, S. Grether-Beck, J. Krutmann, Environment-induced lentigines: formation of solar lentigines beyond ultraviolet radiation, Exp. Dermatol. 24 (6) (2015) 407–411.
[12] J.W. Blunt, B.R. Copp, R.A. Keyzers, M.H. Munro, M.R. Prinsep, Marine natural products, Nat. Prod. Rep. 34 (3) (2017) 235–294.
[13] J. Fitton, D. Stringer, S. Karpiniec, Therapies from Fucoidan: an update, Mar. Drugs 13 (9) (2015) 5920.
[14] A.S. Silchenko, A.B. Rasin, M.I. Kusaykin, A.I. Kalinovsky, Z. Miansong, L. Changheng, O. Malyarenko, A.O. Zueva, T.N. Zvyagintseva, S.P. Ermakova, Structure, enzymatic transformation, anticancer activity of fucoidan and sulphated fucooligosaccharides from Sargassum horneri, Carbohydr. Polym. 175 (2017) 654–660.
[15] A. Mohammed, R. Bissoon, E. Bajnath, K. Mohammed, T. Lee, M. Bissram, N. John, N.K. Jalsa, K.-Y. Lee, K. Ward, Multistage extraction and purification of waste Sargassum natans to produce sodium alginate: an optimization approach, Carbohydr. Polym. 198 (2018) 109–118.
[16] M. DuBois, K.A. Gilles, J.K. Hamilton, P.A. Rebers, F. Smith, Colorimetric method for determination of sugars and related substances, Anal. Chem. 28 (3) (1956) 350–356.
[17] S.F. Chandler, J.H. Dodds, The effect of phosphate, nitrogen and sucrose on the production of phenolics and solasodine in callus cultures of *Solanum laciniatum*, Plant Cell Rep. 2 (4) (1983) 205–208.
[18] K.S. Dodgson, R.G. Price, A note on the determination of the ester sulphate content of sulphated polysaccharides, Biochem. J. 84 (1) (1962) 106–110.
[19] I.P.S. Fernando, K.K.A. Sanjeewa, K.W. Samarakoon, W.W. Lee, H.-S. Kim, N. Kang, P. Ranasinghe, H.-S. Lee, Y.-J. Jeon, A fucoidan fraction purified from Chnoospora minima; a potential inhibitor of LPS-induced inflammatory responses, Int. J. Biol. Macromol. 104 (2017) 1185–1193.
[20] I.P.S. Fernando, T.U. Jayawardena, H.-S. Kim, A.P.J.P. Vaas, H.I.C. De Silva, C.M. Nanayakkara, D.T.U. Abeytunga, W. Lee, G. Ahn, D.-S. Lee, I.-K. Yeo, Y.-J. Jeon, A keratinocyte and integrated fibroblast culture model for studying particulate matter-induced skin lesions and therapeutic intervention of fucosterol, Life Sci. 233 (2019) 116714.
[21] L. Wang, B. Ryu, W.-S. Kim, G.H. Kim, Y.-J. Jeon, Protective effect of gallic acid derivatives from the freshwater green alga Spirogyra sp. against ultraviolet B-induced apoptosis through reactive oxygen species clearance in human keratinocytes and zebrafish, Algae 32 (4) (2017) 379–388.
[22] I.P.S. Fernando, K.K.A. Sanjeewa, H.S. Kim, L. Wang, W.W. Lee, Y.J. Jeon, Apoptotic and antiproliferative properties of 3beta-hydroxy-Delta5-steroidal congeners from a partially purified column fraction of Dendronephthya gigantea against HL-60 and MCF-7 cancer cells, J. Appl. Toxicol. 38 (4) (2018) 527–536.
[23] I. Alim, L. Fadilah Nor Laili, N. Muhammad Trijoko, S. Ratna Asmah, Cytotoxicity of Fucoidan from three tropical Brown algae against breast and Colon Cancer cell lines, Pharmacognosy Journal 9 (1) (2017).
[24] S. Palanisamy, M. Vinosha, T. Marudhupandi, P. Rajasekar, N.M. Prabhu, In vitro antioxidant and antibacterial activity of sulfated polysaccharides isolated from Spatoglossum asperum, Carbohydr. Polym. 170 (2017) 296–304.
[25] R. Daniel, O. Berteau, L. Chevolot, A. Varenne, P. Gareil, N. Goasdoue, Regioselective desulfation of sulfated L-fucopyranoside by a new sulfoesterase from the marine mollusk Pecten maximus: application to the structural study of algal fucoidan (Ascophyllum nodosum), Eur. J. Biochem. 268 (21) (2001) 5617–5626.
[26] S.J. Lim, W.M. Wan Aida, M.Y. Maskat, J. Latip, K.H. Badri, O. Hassan, B.M. Yamin, Characterisation of fucoidan extracted from Malaysian Sargassum binderi, Food Chem. 209 (2016) 267–273.
[27] M.J. Ryu, H.S. Chung, Fucoidan reduces oxidative stress by regulating the gene expression of HO1 and SOD1 through the Nrf2/ERK signaling pathway in HaCaT cells, Mol. Med. Rep. 14 (4) (2016) 3255–3260.
[28] C. Dai, B. Li, Y. Zhou, D. Li, S. Zhang, H. Li, X. Xiao, S. Tang, Curcumin attenuates quinocetone induced apoptosis and inflammation via the opposite modulation of Nrf2/HO-1 and NF-kB pathway in human hepatocyte L02 cells, Food Chem. Toxicol. 95 (2016) 52–63.
[29] I. Mori, Z. Sun, M. Ukachi, K. Nagano, C.W. McLeod, A.G. Cox, M. Nishikawa, Development and certification of the new NIES CRM 28: urban aerosols for the determination of multielements, Anal. Bioanal. Chem. 391 (6) (2008) 1997–2003.
[30] T.A. Davis, B. Volesky, A. Mucci, A review of the biochemistry of heavy metal biosorption by brown algae, Water Res. 37 (18) (2003) 4311–4330.
[31] I.P.S. Fernando, T.U. Jayawardena, K.K.A. Sanjeewa, L. Wang, Y.-J. Jeon, W.W. Lee, Anti-inflammatory potential of alginic acid from Sargassum horneri against urban aerosol-induced inflammatory responses in keratinocytes and macrophages, Ecotoxicol. Environ. Saf. 160 (2018) 24–31.
[32] M.O. Hengartner, The biochemistry of apoptosis, Nature 407 (6805) (2000) 770.
[33] S.-Y. Kim, E.-A. Kim, Y.-S. Kim, S.-K. Yu, C. Choi, J.-S. Lee, Y.-T. Kim, J.-W. Nah, Y.-J. Jeon, Protective effects of polysaccharides from Psidium guajava leaves against oxidative stresses, Int. J. Biol. Macromol. 91 (2016) 804–811.
[34] P. Li, D. Nijhawan, I. Budihardjo, S.M. Srinivasula, M. Ahmad, E.S. Alnemri, X. Wang, Cytochrome c and dATP-dependent formation of Apaf-1/Caspase-9 complex initiates an apoptotic protease cascade, Cell 91 (4) (1997) 479–489.
[35] L.M. Mooney, K.A. Al-Sakkaf, B.L. Brown, P.R.M. Dobson, Apoptotic mechanisms in T47D and MCF-7 human breast cancer cells, Br. J. Cancer 87 (8) (2002) 909–917.
[36] I.P.S. Fernando, K.K.A. Sanjeewa, Y.-S. Ann, C.-i. Ko, S.-H. Lee, W.W. Lee, Y.-J. Jeon, Apoptotic and antiproliferative effects of Stigmast-5-en-3-ol from Dendronephthya gigantea on human leukemia HL-60 and human breast cancer MCF-7 cells, Toxicol. in Vitro 52 (2018) 297–305.

Please cite this article as: I.P.S. Fernando, K.K.A. Sanjeewa, H.G. Lee, et al., Characterization and cytoprotective properties of *Sargassum natans* fucoidan against urban aerosol-induced keratinocyte damage..., , https://doi.org/10.1016/j.ijbiomac.2020.05.132